



Kinetics of photocatalytic, self-cleaning surfaces: A decision tree approach for determination of reaction order

David Ollis*

Chemical and Biomolecular Engineering, North Carolina State University, Raleigh, NC, 27695-7905, United States



ARTICLE INFO

Keywords:
Photocatalyst
Self-cleaning
Kinetics
Power law
Decision table

ABSTRACT

Self-cleaning photocatalytic surfaces have several decades of application, yet satisfactory rate equations for analyzing the kinetics of reactions on such solid surfaces are lacking, due in large part to the many configurations of the catalyst and the deposited contaminants.

We analyze the existing literature and show that nearly all studies can be described by application of the power law for rate of reaction:

$$\text{Rate} = k_{\text{cat}} [\text{C}]^n$$

where n = apparent reaction order, and k_{cat} is a fundamental constant of the catalytic material. The value of reaction order, n , we show requires answers to the following six questions. In each case, the observed apparent kinetic order depends upon interplay among the distributions of photocatalyst, reactant, and irradiance.

1. Is the photocatalyst porous or non-porous?

Example: Stearic acid on/within non-porous/porous photocatalyst layer.

2. Is the photocatalytically active layer optically thin or thick?

Example: Dye conversion in TiO_2 layers vs. 10% $\text{TiO}_2/\text{SiO}_2$?

3. Is the probe reactant deposit a submonolayer or multilayer?

Example: Dye sub/multilayers with TiO_2

4. Is probe reactant light absorption negligible or important?

Example: Stearic acid vs. soot

5. Is the probe reactant present as a continuous film or as a distribution of discrete islands?

Example: Long chain carboxylic acids on TiO_2

6. If distributed, what is breadth of distribution?

Example: Stearic acid on TiO_2

For contaminant removal we demonstrate apparent reaction orders of 0, $\frac{1}{2}$, 1, and 2! Simple analysis is used to explain this diversity of apparent reaction orders. We use the six questions posed to construct a decision tree for determination of the apparent reaction order, n , as a function of responses to the six questions.

1. Introduction

Photocatalyst TiO_2 is able to achieve the total oxidation of a myriad of organic compounds, hence its incorporation into a number of self-cleaning surface products, including transparent, non-porous window and automotive glasses, opaque ceramic tiles, paints, as well as porous cementitious building materials and paving blocks [1,2]. Pioneering labs exploring self-cleaning photocatalysts include those of Mills, Parkeins, Daoud, Fujishima, Motazer, Karii, and Kiwi, the last of whom is the researcher to whom this volume of Applied Catalysis B is dedicated.

The earliest “self-cleaning” photocatalyst paper identified through Web of Science by searching (photocat* and self-cleaning) is titled

“Photocatalyzed oxidation of crude oil residue by beach sand” by Wise and Sancier [3a]. Their 1991 data (Table 1) indicates a wavelength dependence of the photo-oxidation rate. The substantially higher rate observed when near UV (< 400 nm) photons were used suggests photocatalysis as the dominant mechanism for the observed oxidation of carbonaceous residue. The metal oxide phases identified (magnetite Fe_2O_3 , ilmenite FeTiO_3) have semiconductor bandgaps in the visible.

Support exists for ilmenite as a photoactive component of beach sand. Ilmenite has been reported to be a photocatalyst for dechlorination of carbon tetrachloride [3b] and mineralization of dichloroacetic acid [3c] in water. A TiO_2 coating enriched by FeTiO_3 had enhanced activity for gas phase acetaldehyde oxidation [3d], and an ilmenite

* Corresponding author.

E-mail address: ollis@ncsu.edu.

Table 1Effect of wavelength on photo-oxidation rate^a [3a].

Wavelength (nm)	CO ₂ Production Rate (mol m ⁻² h ⁻¹) × 10 ³
All (hp mercury lamp)	2.6
> 480	0.7
> 620	0.4

^a Beach sand from Fort Funston, CA.**Table 2**

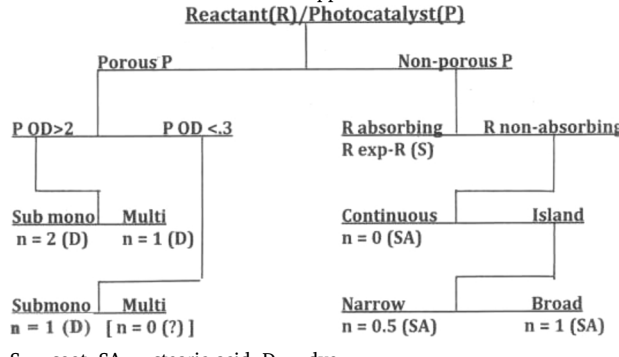
Papers for (Photocat* + Self-cleaning) surfaces.

(Web of Science, 6/29/2018)

2018	98(partial)
2017	193
2016	143
2015	142
2014	140
2013	131
2012	94
2011	96
2010	74
2009	69
2008	55
2007	35
2006	26
2005	14
2004	14
2003	11
2002	8
2001	5
2000	9
1999	6
1998	4
1997	1
...	
1991	1

Table 3

Decision tree for determination of apparent reaction order.



S = soot, SA = stearic acid, D = dye.

(FeTiO₃) nanodisc/TiO₂ composite was 25X times more active than the reference photocatalyst, Degussa P25, for 2-propanol photocatalyzed oxidation [3e].

Since 1991, the literature on self-cleaning surfaces has grown considerably, especially in the last decade. From 1991 to 2018, a Web of Science search identifies > 1300 related papers, indicating a rapidly growing interest evident from Table 2.

The self-cleaning properties of titania-based photocatalysts have been reviewed extensively in recent years; Web of Science identifies at least 67 reviews in the interval 2002–2018, including those of Zhang [4a], Banerjee [4b], and McGuiness [4c]. Among the many topics discussed including activity, composition, hydrophilicity/hydrophobicity, and contact angle, kinetic models were notably absent. This circumstance is surprising, since the central aspect of catalysis is kinetics.

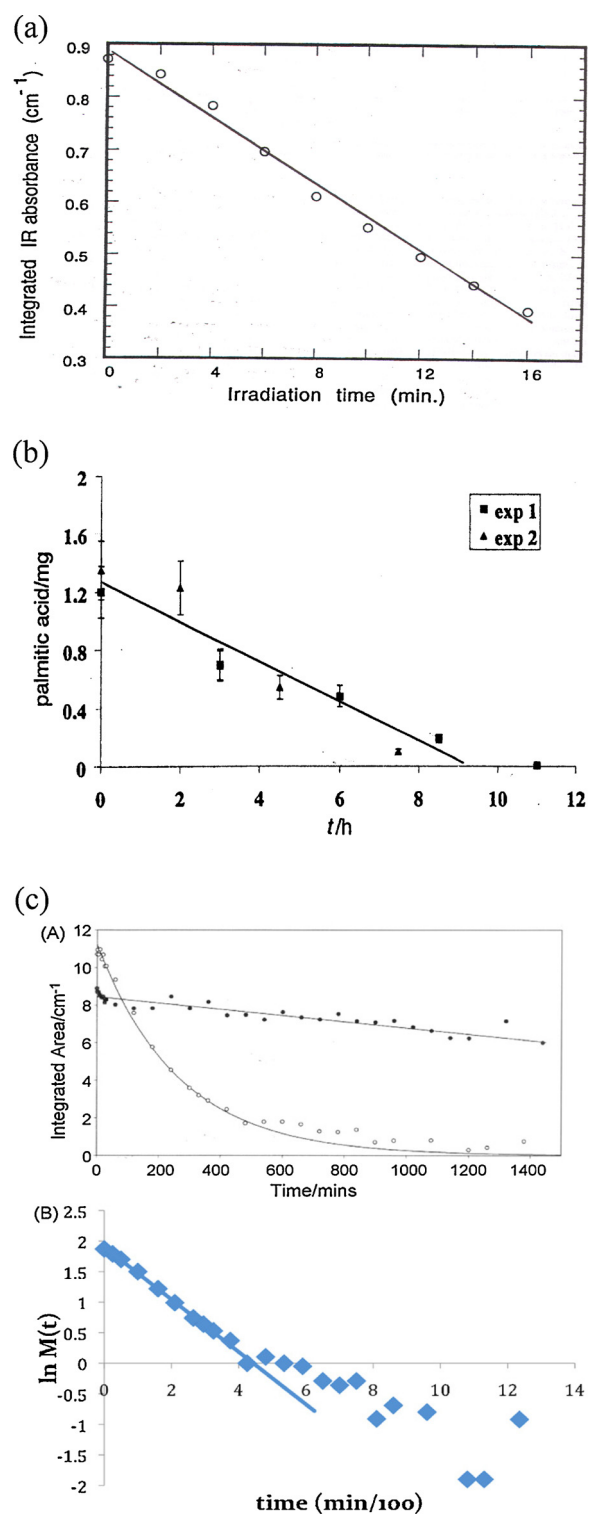


Fig. 1. (a) Integrated 2700–3000 cm⁻¹ IR stearic acid absorbance vs. time (TiO₂ film on glass, 365 nm, I = 2.4 mW/cm²) [5] (Reprinted by permission of Cambridge University Press). (b) Mass of palmitic acid (and intermediates) vs. time [6] (Reprinted by permission of Royal Society of Chemistry). (c) Integrated IR spectrum (2700 cm⁻¹–3000 cm⁻¹) vs. time for two photocatalysts: Activ (solid circles) and Degussa P-25 (open circles) [7]. Note zero order behavior for Activ non-porous photocatalyst vs. first order (solid curve) for Degussa porous film [7] (Reprinted by permission of Elsevier).

However, as the fundamental mechanism(s) for oxidative behavior of photocatalytic self-cleaning surfaces for removal of organic deposits remains unclear, the lack of kinetic models is understandable, if

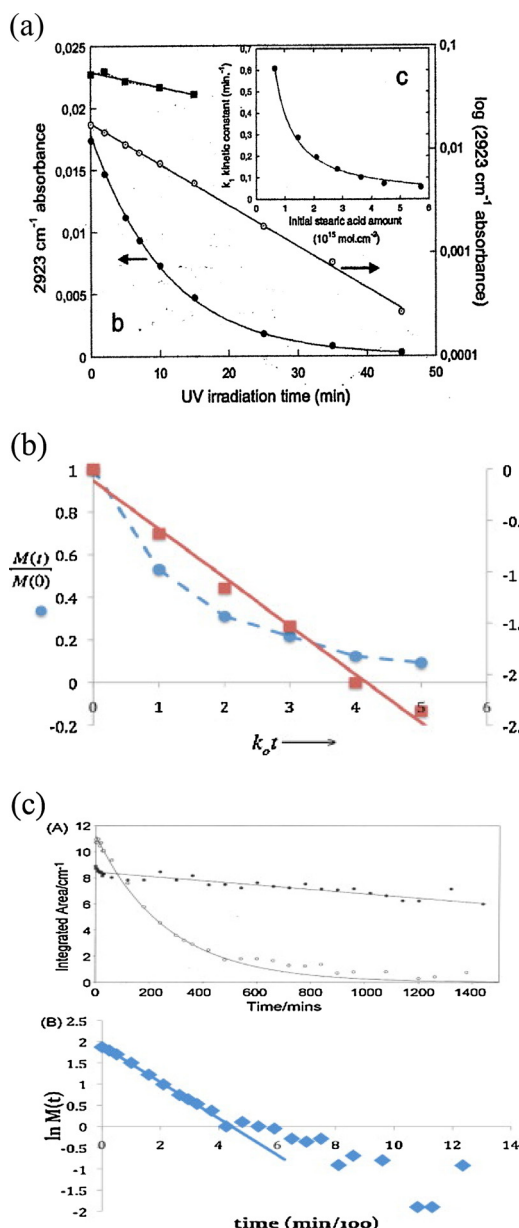


Fig. 2. (a) Evolution of 2923 cm^{-1} IR signal for mesoporous (circles) and microporous (squares) photocatalyst. Mesoporous data plotted as IR and $\log(\text{IR})$, showing first order fit, vs. microporous catalyst data showing zero order kinetics. Insert: Apparent first order rate constant (min^{-1}) vs. initial stearic acid loading ($\times 10^{15}$ molec/cm 2) [8] (Reprinted by permission of Wiley-VCH). (b) Model calculations for stearic acid photocatalyzed oxidation. Remaining mass (blue circles) and $\ln(\text{mass})$ (red squares) vs time, showing apparent first order behavior [9]. (Reprinted by permission of Elsevier) (For interpretation of the references to colour in this figure legend, the reader is referred to the web version of this article).

regrettable. The present paper summarizes recent kinetic models (Ollis (2010, 2015)) to create a new analytical structure, namely a decision tree, for pre-determination of reaction order, n , for the empirical power law form, $\text{rate} = k C^n$ which we have shown to fit data from more than 30 papers for a range of photocatalysts (porous, non-porous; high and low optical density), organic deposit configurations (continuous film, discrete islands or ridges), and reactants (transparent or absorbing for near UV). Since this set of circumstances covers many of the more than 1300 articles published to date on self-cleaning photocatalysts, we propose that utilization of this organizing principle, based upon physically meaningful circumstances important in kinetics (catalyst

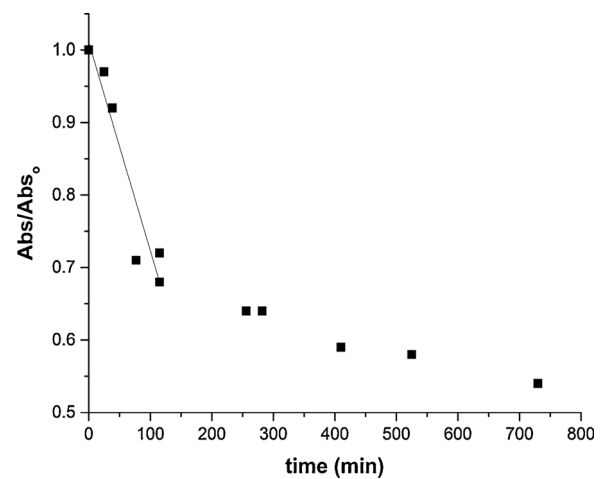


Fig. 3. Normalized absorbance for Reactive Black 5 vs. time (Data from Fig. 7 of [10] showing apparent zero order for first 33% conversion).

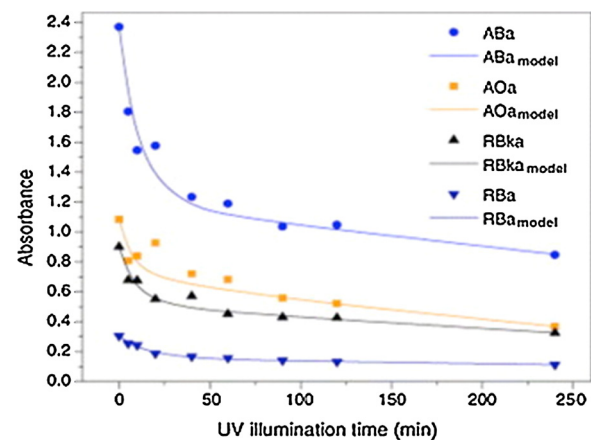


Fig. 4. Absorbance vs. time for photocatalytic oxidation of dye submonolayers on porous TiO_2 films of dyes Reactive Black 5 (RB5), Reactive Blue 19 (RB19), Acid Blue 9 (AB9), and Acid Orange 7 (AO7) [11].

porosity and optical density, contaminant deposit form (continuous film vs discrete islands or ridges), island size distribution, and reactant optical density, will lead to progress in understanding the many kinetic behaviors exhibited by such catalysts. The classification presented here involves simple catalyst configurations (porous or non-porous) of pure TiO_2 and a single $\text{TiO}_2/\text{SiO}_2$ composite example. Thus, analysis of more complex circumstances such as photocatalysts deposited in turn on or within membranes, inorganic or organic fibers and textiles, porous construction materials, etc., are excluded here, but invite future analyses.

This paper summarizes key results dealing with the kinetics of organic deposit removal from photocatalytic, self-cleaning films deposited on flat, non-porous supports, identifies the (apparent) order of photocatalyzed reaction in each case, and proposes a universal decision table for prediction of reaction order. The self-cleaning photocatalysis literature includes oxidative removal of long chain fatty acids [5–9], organic dyes [12], soot [15–17], bacteria [21], and even coffee stains [22]. We organize these results to show that the apparent kinetics of organic film removal can be described by an empirical rate form (Eq. 1), known generally as the power law,

$$\text{Rate} = k_{\text{cat}} (X)^n \quad (1)$$

where X = measurable variable reflecting the reactant concentration or mass on the local photocatalyst surface, and n = apparent reaction order, and k_{cat} is a rate constant which does not vary with X .

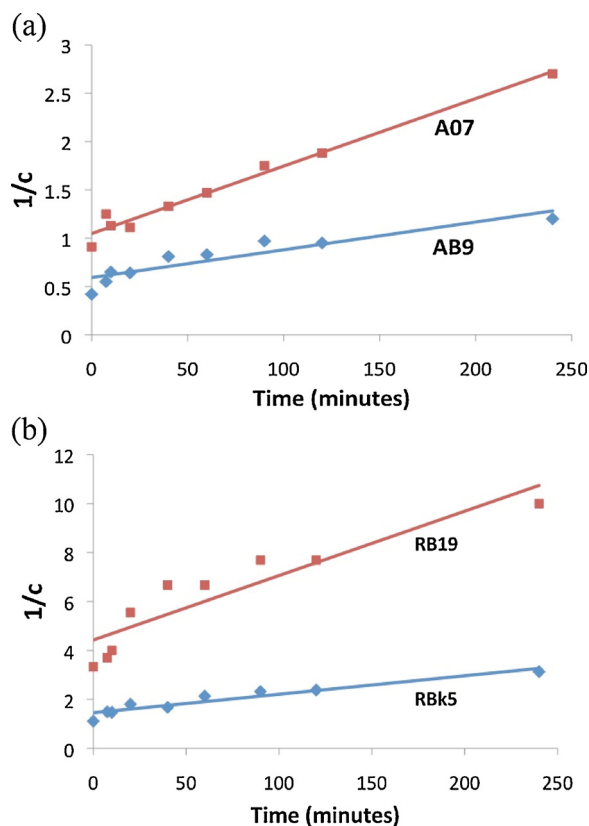


Fig. 5. (a, b) Plots of reciprocal dye concentrations vs. time for same data as **Fig. 4**, showing linearity of 3 out of 4 dyes, indicating apparent second order behavior (Reprinted by permission of Elsevier).

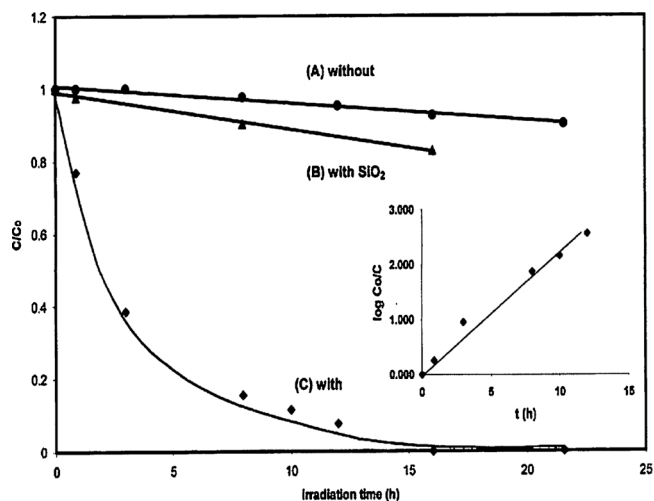


Fig. 6. Decolorization of Indigo Carmine solid particles mixed with nothing (a), SiO_2 (B) and TiO_2 particles (C) vs. time. Insert shows apparent first order behavior [13]. (Reprinted by permission of Elsevier).

We argue that the best way to compare photocatalysts is by comparison of rate constants, k_{cat} . We demonstrate that the appropriate value of reaction order, n , is needed to usefully analyze experimental results, i.e., to obtain a rate constant, k_{cat} , which does not vary with variable X. We show that determination of this apparent reaction order depends upon the answers to six fundamental questions:

- 1 Is the photocatalyst non-porous or porous, i.e., does it allow deposition of the reactant into the catalyst pores, or only on the

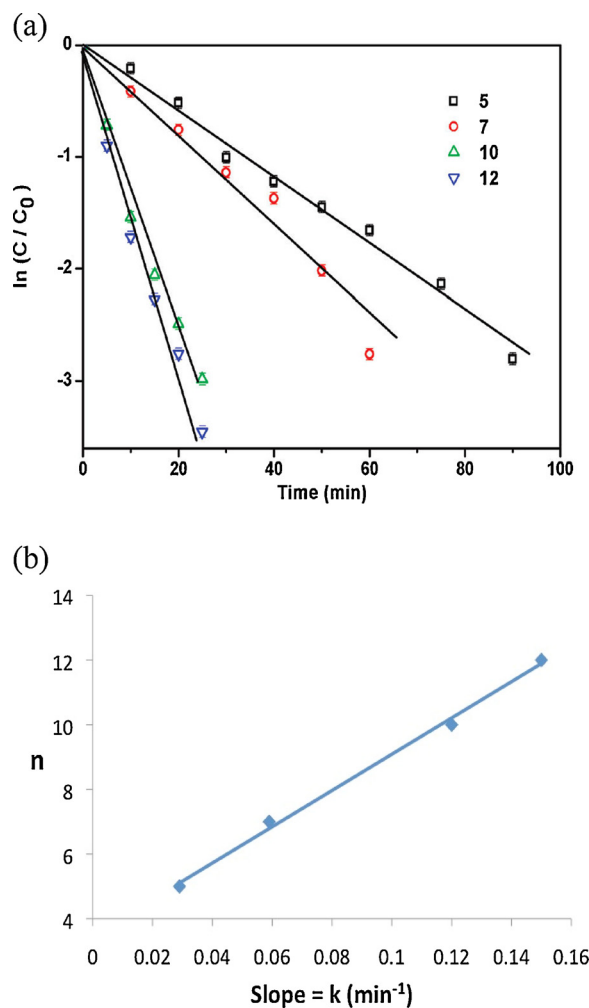


Fig. 7. (a) Semilog plot of $\ln(C(t)/C_0)$ for dye RB9 on composite photocatalyst containing poly (diethyldiammonium chloride) (PDDA), poly-sulfonated polystyrene(PSS), silica (SiO_2) and TiO_2 [14]. Number of deposited composite photocatalyst layers were 5 (squares), 7 (circles), 10 (triangles) and 12 (inverted triangles) (Reprinted by permission of American Chemical Society). (b) Number of composite photocatalyst layers vs. observed rate constant, k (min^{-1}) [12] (Reprinted by permission of Elsevier).

external catalyst surface?

- 2 If porous, is the photocatalyst layer optically thin ($\text{OD} < 0.3$), providing essentially uniform illumination throughout the porous catalyst layer, or is it optically thick ($\text{OD} > 2$), in which case illumination, and thus local reaction rate, varies strongly within the catalyst layer?
- 3 Is the reactant initially deposited as a sub-monolayer or as a multilayer?
- 4 Is absorption of the incident near-UV or UV light by the reactant important (example: soot) or unimportant (example: stearic acid), i.e., does reactant compete with the photocatalyst for photons?
- 5 Is the reactant deposit in the form of a continuous film, or that of discrete islands, particles, or ridges, etc.?
- 6 If the organic deposit is in discrete form, is the size distribution of its islands, ridges, etc., monodisperse, narrow, or broad?

As these questions are framed to be answered only as YES or NO, we collect responses in the form of a decision tree, which will provide a rational choice of apparent reaction order, n , based upon multiple literature results and some elementary kinetic arguments.

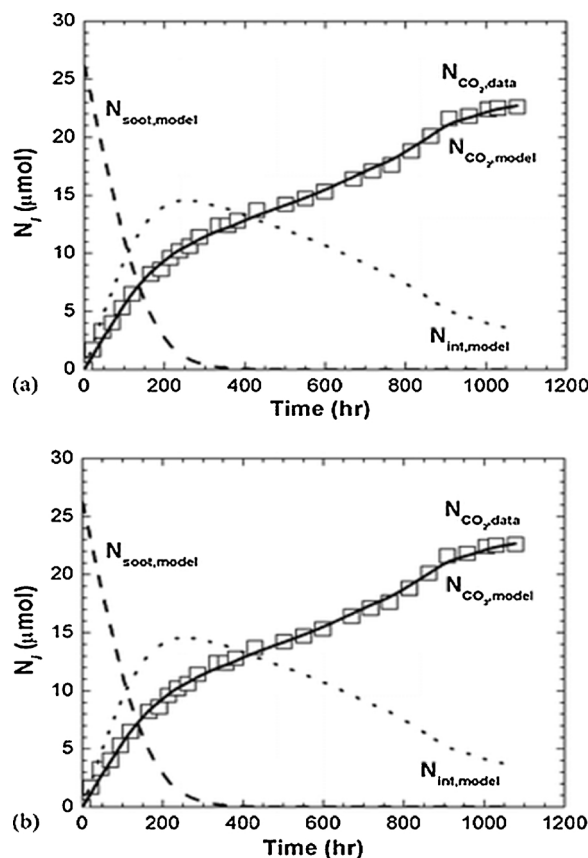


Fig. 8. Photocatalyzed oxidation of soot on Activ™ glass. Data vs. model for soot, soot intermediate, and CO_2 vs time. CO_2 data (squares) vs model (curve) [16]. (Reprinted by permission of American Chemical Society).

2. Results and discussion

It is convenient to present the decision tree first (Table 3) as our working hypothesis. We will establish its validity through testing literature examples against the six questions above. This tree indicates that for a photocatalyzed self-cleaning reaction, the apparent order observed, n , ranges from 0 to 2. The ultimate goal of this paper is to argue for use of such a decision tree table for predicting the apparent kinetic order, n , and thus determination of catalyst activity, k_{cat} .

2.1. Question 1: porous or non-porous photocatalyst surface?

Early reports (Paz [5], Romeas [6], and Mills [7]) for photocatalyzed oxidation of stearic [5,7] or palmitic [6] acid on non-porous TiO_2 thin films, especially Pilkington's "Activ" glass, showed a clearly zero order behavior by plotting IR peak intensities of $-\text{CH}_2-$ groups in the residual fatty acid (stearic (SA), palmitic (PA)) and intermediates vs. time (Fig. 1a–c (solid data points)).

2.2. Question 2: is photocatalyst porous?

However, when porous photocatalysts were used, Mills [7] and Allain [8] observed an apparent first order behavior for SA disappearance (Figs. 1c (open circles), 2). Ollis [9] interpreted this behavior as due to a zero order local oxidation rate for a reaction whose local light intensity, and thus rate constant, k_{cat} , varied with depth into the porous catalyst layer. A kinetic disguise thus was demonstrated in which a non-uniform illumination field in a porous catalyst increased the apparent reaction order from $n = 0$, for stearic acid multilayers (Figs. 1a–c) on a non-porous surface, to $n = 1$ for the same reactants deposited as multilayers within a porous catalyst (Figs. 1c (bottom) and

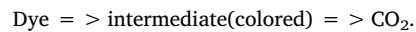
2 a). His model calculation for a 5 layer porous catalyst with exponential decrease with depth of intensity, and thus rate constant, demonstrated a kinetic disguise: a local zero order reaction exhibited an overall apparent first order behavior (Fig. 2b).

2.3. Question 3: reactant deposited as submonolayer or multi-layers?

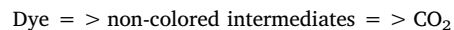
Stearic acid multilayer deposits on non-porous active glass exhibited a zero order kinetics (Fig. 1c (solid circles); this same reaction was carried out to at least 65% conversion (Fig. 1a) on a TiO_2 film on glass.

Similarly, dye multi-layers on a non-porous, optically thin TiO_2 layer (Activ glass) appears to show zero order kinetics up to 30% conversion, as indicated by the linear plot (Fig. 3) of residual dye IR peak intensity vs. time [10]. Here, the uniform illumination on the nonporous catalyst surface meant that the rate constant, k_{cat} was everywhere characterized by a single intensity, I_o , and no kinetic disguise arose as a result of non-uniform illumination.

Porous photocatalysts used to degrade organic dyes also displayed a kinetic disguise in air-solid systems. We earlier [11] interpreted kinetics of dye submonolayer oxidation on illuminated TiO_2 powders (Fig. 4) as indicative of a serial reaction:



However, our subsequent stearic acid/palmitic acid modeling paper [9] caused us to reinterpret [12] the previous submonolayer dye oxidation kinetics as a disguise in which a presumably first order reaction



would fit a second order disguise, again due to a non-uniform intensity profile within the porous photocatalysts [12]. A second order reaction rate form,

$$dC/dt = k C^2,$$

integrates to provide

$$1/C - 1/C_0 = -kt$$

This latter behavior was demonstrated by the linearity of plots of reciprocal concentration vs. time, as shown for three of the four dyes investigated earlier (Fig. 5a–d) [12].

The same disguise occurs for dye "multi-layers" within a porous, high optical density (OD) system, that of finely ground solid indigo mixed with TiO_2 powder. This "multilayer" reactant configuration would be expected to exhibit intrinsic, zero order bleaching kinetics (constant surface coverage over most time), but the global kinetics show an apparent first order behavior (Fig. 6, inset) [13]. Again, as with stearic acid multilayers, light absorption within the high OD porous catalyst layers causes a kinetic disguise, increasing the apparent reaction order from $n = 0$ to $n = 1$ for dye multilayers within a porous catalyst, and from $n = 1$ to $n = 2$ for dye submonolayers within such catalysts.

If this variable intensity disguise is correct, then a porous, optically thin ($OD < 0.3$) catalyst should exhibit intrinsic kinetics. This predicted behavior is shown in Fig. 7a, in which sub-monolayers of dye distributed within a porous TiO_2 – SiO_2 photocatalyst, created by successive dip coats of a slurry, exhibit intrinsic first order behavior [14]. The uniformity of illumination, hence low optical density, is demonstrated by plotting the apparent first order rate constant (slopes in Fig. 7a) vs. number of dip coat layers deposited (Fig. 7b). Each layer increases the overall rate constant, k , value by the same absolute amount, hence light intensity must have been uniform throughout this porous catalyst, as each layer is equally active.

2.4. Question 4: reactant absorbing or transparent?

The presence of a light absorbing reactant, deposited on top of a

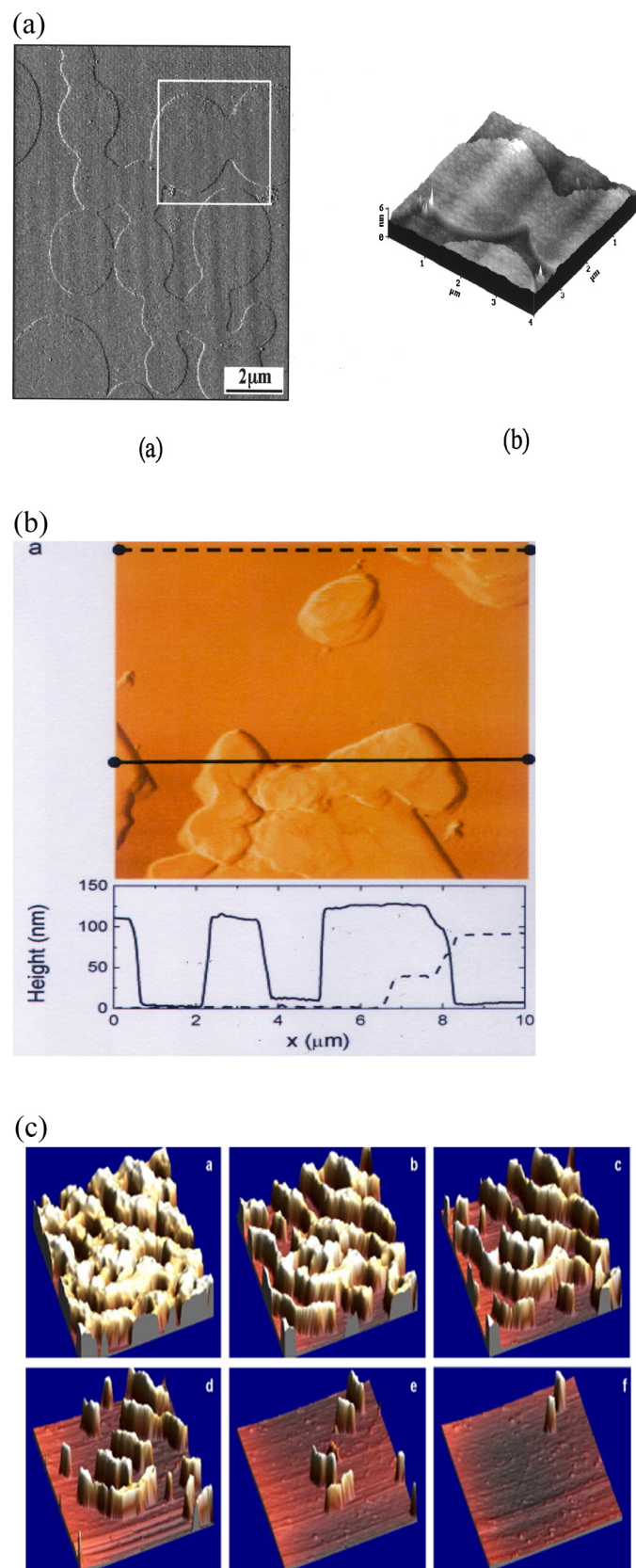


Fig. 9. (a) AFM image of partial stearic acid film on single crystal rutile (110) surface. Island height is $2.13 +/ - 0.12$ nm, vs 2.5 nm for length of fully extended SA molecule [18]. (Reprinted by permission of American Chemical Society). (b) AFM image of SA deposits on titania film. Height profile vs. distance for solid line through image in Fig. 9a [19]. (Reprinted by permission of Elsevier).

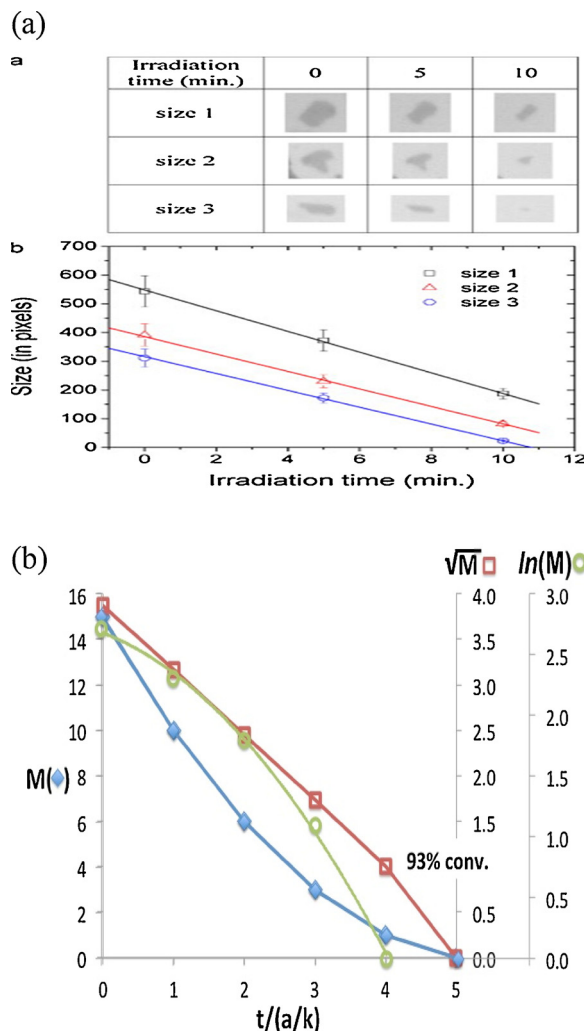


Fig. 10. (a) Microscopy images and (b) island area (pixels) vs. time for stearic acid photocatalyzed oxidation [19]. (Reprinted by permission of Elsevier). (b) Calculated total area $A(t)$ vs. time for assumed reaction orders $n = 0$ (blue diamonds), $n = 1/2$ (red squares) and $n = 1$ (yellow green circles). The value $n = 0.5$ provides the apparent reaction order [23]. (Reprinted by permission of Elsevier). (For interpretation of the references to colour in this figure legend, the reader is referred to the web version of this article).

photocatalyst, would be expected to reduce the illumination reaching the photocatalyst, and hence reduce the photon-driven rate. Progressive removal of such a reactant layer would increase the photon flux reaching the catalyst surface, and thus also increase the rate constant. The PCO of soot removal is an example of such behavior (Fig. 8a). Here, the measured CO_2 generation we modeled as the parallel/serial network of reactive and recalcitrant soot components [16]:



and



The data shows that no simple kinetic order suffices, as rate decreases due to decreasing soot concentrations (mass action law), but increases with diminishing soot thickness due to increasing light transmission. This conflict is represented by a kinetic term of the form $(R) \exp(-R/a^d)$ where d = effective soot layer thickness a = specific absorbance coefficient for soot and R = soot mass. This case appears in Table 1 under the category (non-porous P , absorbing R), and represents the sole case where the simple power law (Eq. (1)) does not fit.

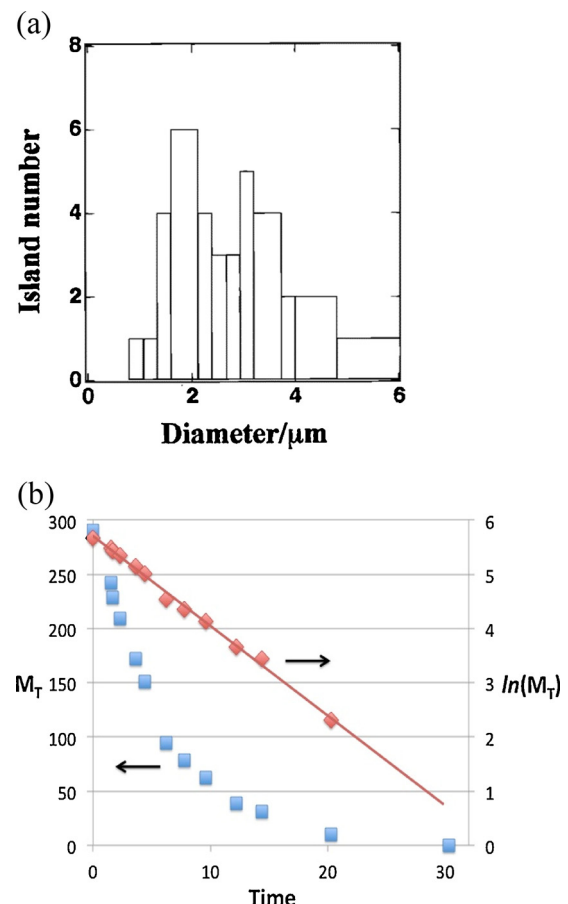


Fig. 11. (a) Island size distribution for stearic acid submonolayer deposit on TiO_2 (110) single crystal surface of $20\mu\text{m} \times 20\mu\text{m}$ area. [18]. (Reprinted by permission of American Chemical Society). (b) Calculated mass (area) vs. time plotted as $M(t)$ and $\ln(M_t)$. Straight line for $n = 1$ indicates apparent first order reaction for broad distribution shown in Fig. 11a [23]. (Reprinted by permission of Elsevier).

Smits et al [17a, b] have reported success in using the our kinetic model to fit their photocatalyzed soot oxidation results, as shown in Fig. 8b.

2.5. Question 5: initial deposit is continuous film or discrete particles?

Early studies of stearic acid (SA) multilayer photocatalyzed oxidation [5–8] showed kinetics which could be modeled as progressively thinner continuous layers on either non-porous or porous TiO_2 [9], as judged by the convenient measure of IR signal from residual $-\text{CH}_2-$ groups. These models were derived assuming uniform initial and residual multilayers on or within the catalysts, and fit IR data well ($n = 0$, Figs. 1a–c and $n = 1$, 2 a,b)).

2.6. Question 6: size distribution of reactant is monodisperse, narrow, or broad?

This assumption of progressive thinning of a continuous overlayer was not always valid. Other reports using atomic force microscopy (AFM) and optical microscopy to examine fatty acid deposits on single crystals of anatase [18] and rutile [20] as well as polycrystalline titania films [19] revealed discontinuous deposits of various forms, including uniformly thin, circular islands (Fig. 9a), multilayer islands of variable height (Fig. 9b) or even similarly spaced ridges of uniform initial height (Fig. 9c). Visual measurements of individual SA island area vs. time on single crystals of anatase TiO_2 (Fig. 10a) showed a zero order behavior:

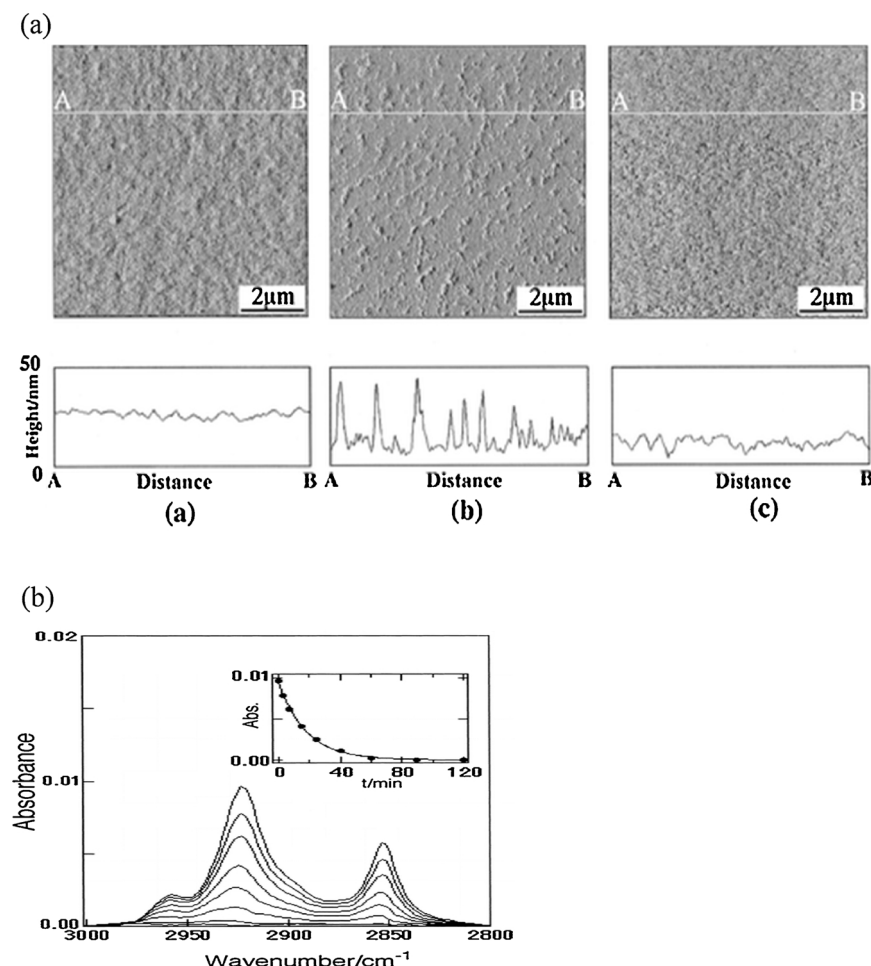


Fig. 12. (a) AFM images (top) and height profile (bottom) of SA Langmuir–Blodgett (LB) layers deposited on TiO₂ films [24] (Reprinted by permission of American Chemical Society). (b) Absorbance vs. time for five layer stearic acid LB film deposited on anatase layer. Insert shows fit to first order model [24] (Reprinted by permission of American Chemical Society).

Island area removal rate was essentially constant independent of island size, thus each island disappeared following zero order kinetics, the same as a continuous SA film would provide.

The non-uniform island sizes are evident from the microscopy photos of Sawunyama [18] and Ghazzal [19]. Such island size distributions led to early disappearance of the smallest islands, and later of other, larger islands, and a kinetic disguise may again be expected, as we established previously [12].

For example, consider a five island model with initial values of island area a_i , where the size distribution is given by multiples of the smallest size, a . Thus the island sizes, a_1 through a_5 , are taken as the following distribution:

$$a_1 = a, a_2 = 2a, a_3 = 3a, a_4 = 4a, \text{ and } a_5 = 5a.$$

The disappearance kinetics of constant rate regardless of island size (Fig. 10a) give the model for individual island area as

$$a_1 = a - kt$$

$$a_2 = 2a - kt$$

$$a_3 = 3a - kt$$

$$a_4 = 4a - kt$$

$$\text{and } a_5 = 5a - kt$$

The total area, $A(t)$, can be calculated at different time intervals from the areas of the individual islands. Thus we model $A(t)$ as the sum

of all island areas:

$$A = (a + 2a + 3a + 4a + 5a) - 5kt = 15 - 5kt \quad 0 < t < a/k$$

$$A = (2a + 3a + 4a + 5a) - 4kt = 14a - 4kt \quad a/k < t < 2a/k$$

$$A = (3a + 4a + 5a) - 3kt = 12a - 3kt \quad 2a/k < t < 3a/k$$

$$A = (4a + 5a) - 2kt = 9a - 2kt \quad 3a/k < t < 4a/k$$

$$A = (5a) - kt \quad 4a/k < t < 5a/k$$

$$A = 0 \quad 5a/k < t$$

Plots of $A(t)$ vs t will thus exhibit a constantly diminishing local slope (coefficient of t). Plots of calculated A vs t (Fig. 10b) assuming zero, half, and first order kinetics show that a half-order kinetics ($n = 1/2$) fits the model calculations better than either a zero order or first order model. This distribution of assumed island sizes we will term "narrow", i.e., the ratio of largest to smallest island areas is 5, thus the ratio of diameters is $(5)^{0.5} =$ only 2.24. Such a result indicates that the island size distribution affects the apparent reaction order.

A broader distribution of island sizes was measured by Sawunyama (Fig. 11a) for stearic acid partial monolayers on TiO₂ (110) crystal face. Using the same island kinetics as above, now for the diameters 1–6 μm, thus area ratios of 36, the island size distribution noted in Fig. 11a (12 sizes; 36 islands) provides a linear plot for $\ln [A(t)]$ vs t , which showing an apparent first order behavior (Fig. 11b), in agreement with the experimental data (inset, Fig. 11c). Hence, we conclude that apparent

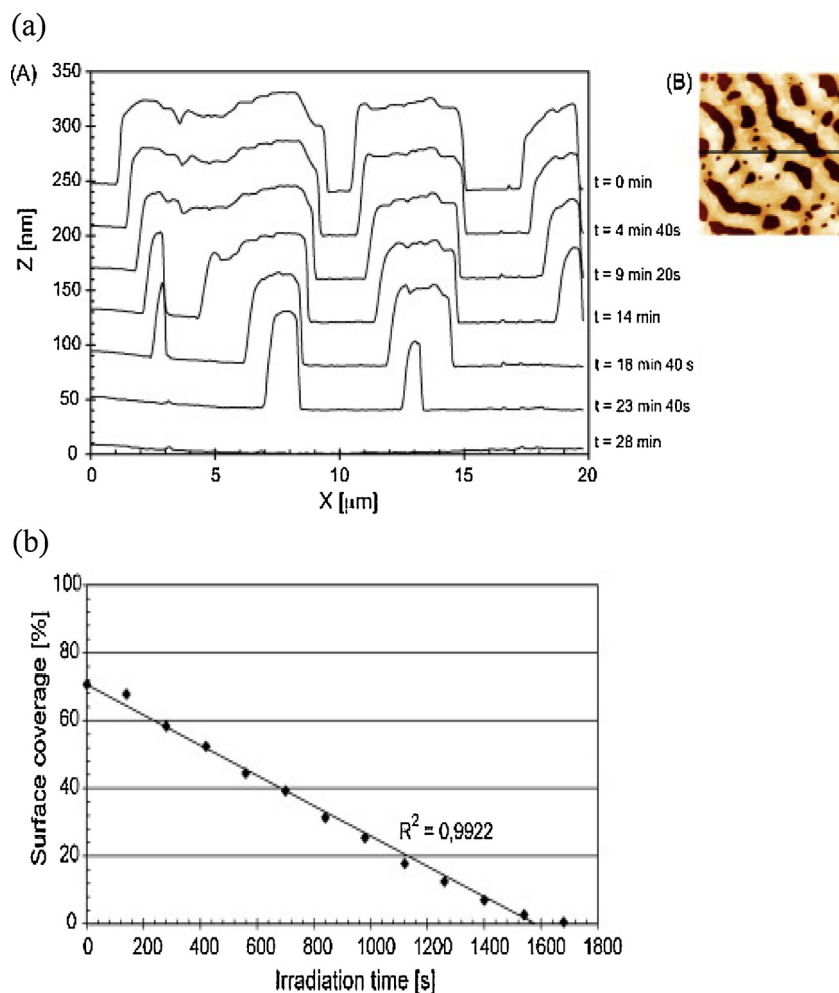


Fig. 13. (a) AFM traces vs. time for lauric acid photocatalyzed removal from anatase single crystal surface [20] (Reprinted by permission of Elsevier). (b) Percent surface coverage by lauric acid on surface of Fig. 13a [20]. (Reprinted by permission of Elsevier).

reaction order depends on island initial size distribution as follows:

monodisperse = $> n = 0$

narrow distribution = $> n = 0.5$

Broad distribution = $> n = 1$

as shown in the bottom right portion of the proposed decision tree. (Table 1)

A second intriguing example is shown by the disappearance rate of the lauric acid ($\text{C}_{12}\text{H}_{24}\text{O}_2$) uniform ridges on the TiO_2 single crystal (orientation unknown), Fig. 9c. If we imagine such uniform ridges as elongated islands, we might expect a zero order rate of disappearance, as was indeed observed when the surface coverage observed by microscopy was used as the basis for extent of lauric acid destruction. (Fig. 12b).

3. Conclusions

In summary, kinetic rate analysis of self cleaning, photocatalytic surfaces illustrates that a single rate equation of the power law form

$$\text{rate} = k_{\text{cat}} (X)^n$$

where X represents a measure of (residual) reactant, can be used to fit data derived from measures of reactant levels (methylene IR peak heights, reactant mass(soot), dye IR peaks, or island size). A singular exception occurs for optically dense reactant (soot) deposited on TiO_2

as followed by CO_2 evolution; this case was modeled in terms of residual reactant (R) by the form below:

$$\text{rat} = k_1 (R_1) \text{ (reactive)} + k_2 (R_2) \exp(-R_2 d) \text{ (recalcitrant)}$$

where d = soot layer depth, and the soot is assumed to be composed of rapidly oxidized volatiles R_1 , designated (reactive) and mostly non-volatile (char) component R_2 (recalcitrant) which oxidized more slowly [16].

Using literature experimental data for photocatalytic self cleaning surfaces, we have validated our opening hypothesis, shown in Table 3, namely, that an appropriate decision tree model can both categorize, and through simple models, rationalize the observed variation in apparent reaction order, n , with circumstance.

The advantages of this approach include:

- (1) The model circumstances assumed (submonolayer vs multilayers, porous vs. non-porous, continuous vs. island deposits, absorbing vs. non-absorbing reactants, optically dense vs. optically thin photocatalysts) describe most of the extant literature. Thus our kinetic approach should be broadly applicable.
- (2) The structure of the decision table suggests that the reaction order can now be predicted in advance, provided one can answer the six questions posed earlier prior to beginning an experiment. This assertion needs wider testing as most systems presented here involve a single example or two.
- (3) The nature of the analysis should be applicable to photosensitized

as well as photocatalyzed systems. [12] Where it occurs, (homogeneous) photolysis could be included as well.

We can now argue that the kinetics of self-cleaning photocatalytic surfaces is beginning to be seriously organized so that our understanding may progress.

Acknowledgement

This work was supported by the State of North Carolina.

References

- [1] Y. Ohama, D. Van Gemert, Application of Titanium Dioxide Photocatalysis to Construction Materials, Springer, 2011.
- [2] V. Augugliaro, et al., Clean by Light Irradiation: Practical Applications of Supported TiO₂, RSC Publishing, 2010.
- [3] (a) H. Wise, L. Sancier, *Catal. Lett.* 11 (1991) 277–284 (A preliminary report of this research appeared in *Atmospheric Environment*, 15 (1981) 639–640, but did not mention the self-cleaning possibility);
 (b) M. Schoonen, Y. Xu, D. Strongin, *J. Geochem. Explor.* 62 (1998) 201–205;
 (c) N. Smirnova, A. Eremenko, O. Rusina, *J. Sol-Gel Sci. Tech.* 21 (2003) 109–113;
 (d) F. Xe, T. Tsumura, K. Nakata, A. Ohmori, *Mat.Sci. Eng. B* 148 (2008) 154–161;
 (e) Y. Kim, B. Gao, S. Han, M. Jung, A. Chakraborty, T. Ko, C. Lee, W. Lee, *J. Phys. Chem. C* 113 (2009) 19179–19184.
- [4] (a) L. Zhang, R. Dillert, D. Bahnemann, M. Vormoor, *Energy Environ. Sci.* 5 (2012) 7401–7507;
 (b) S. Banerjee, D. Dionysios, S. Pillai, *App. Catal. B: Environ.* 176–177 (9) (2015) 396–342;
- [c] N. McGuiness, et al., Self- cleaning Photocatalytic Activity: Materials and Application, in: D. Dionysiou, G. Li Puma, J. Ye, J. Schneider, D. Bahnemann (Eds.), *Photocatalysis: Applications*, RSC Energy and Environment Series No. 15, 2016, pp. 204–235 Chapter 8.
- [5] Y. Paz, Z. Luo, L. Rabenberg, A. Heller, *J. Mater. Res.* 12 (1995) 2842–2848.
- [6] V. Romeas, P. Pichat, C. Guillard, T. Chopin, C. Lehaut, *New J. Chem.* 23 (1999) 365–373.
- [7] A. Mills, A. Lepre, N. Elliott, S. Bhopal, I. Parkin, S.J. O'Neill, *Photochem. Photobiol.* A 160 (2003) 213.
- [8] E. Allain, S. Besson, C. Durand, M. Moreau, T. Gacoin, J.-P. Bollot, *Adv. Funct. Mater.* 17 (2007) 549–554.
- [9] D. Ollis, *Appl. Catal. B* 99 (2010) 478.
- [10] P. Chin, D. Ollis, *Catal. Today* 123 (2007) 177–188.
- [11] A. Julson, D. Ollis, *Appl. Catal. B* 65 (2006) 315.
- [12] D. Ollis, *Appl. Catal. B Environ.* 165 (2015) 111–116.
- [13] M. Vautier, C. Guillard, J.-M. Herrmann, *J. Catal.* 201 (2001) 46.
- [14] H.L. Wang, Y. Hu, L. Zhang, C. Li, *Ind. Eng. Chem. Res.* 3654 (2010) 3662.
- [15] A. Mills, J. Wang, M. Crow, *Chemosphere* 64 (2006) 1032–1035.
- [16] P. Chin, G. Roberts, D. Ollis, *Ind. Eng. Chem. Res.* 46 (2007) 7598–7604.
- [17] M. Smits, C. Chan, T. Tytgat, B. Craeye, N. Costarramone, S. Lacombe, S. Lenaerts, *Chem. Eng. J.* 222 (2013) 411.
- [18] P. Sawunyama, A. Fujishima, K. Hashimoto, *Langmuir* 15 (1999) 3551.
- [19] M. Ghazzal, N. Barthen, N. Chaoii, *Appl. Catal. B* 103 (2011) 85.
- [20] A. Zaleska, J. Nalaskowski, J. Hupka, J. Miller, *Appl. Catal. B* 88 (2009) 407.
- [21] E. Wolfrum, J. Huang, D. Blake, P.-C. Maness, Z. Huang, J. Fiest, W. Jacoby, *Environ. Sci. Technol.* 36 (2002) 3412–3419.
- [22] A. Heller, *Acc. Chem. Res.* 28 (1995) 503–508.
- [23] D. Ollis, *Appl. Catal. B Environ.* 209 (2017) 174–183.
- [24] P. Sawunyama, L. Jiang, A. Fujishima, K. Hashimoto, *J. Phys. Chem. B* 101 (1997) 11000–11003.